De novo missense variant in the GTPase effector domain (GED) of *DNM1L* leads to static encephalopathy and seizures

Nurit Assia Batzir[1,†], Pranjali K. Bhagwat[1,2,†], Tanya N. Eble[1], Pengfei Liu[1,3], Christine M. Eng[1,3], Sarah H. Elsea[1,3], Laurie A. Robak[1,2], Fernando Scaglia[1,4], Alica M. Goldman[1], Shweta U. Dhar[1,5,*] and Michael F. Wangler[1,2,*]

[1]Department of Molecular and Human Genetics, Baylor College of Medicine, Houston TX 77030, USA, [2]Neurological Research Institute, Texas Children's Hospital, Houston TX 77030, USA, [3]Baylor Genetics, Houston, TX 77021 USA, [4]BCM-CUHK Center of Medical Genetics, Prince of Wales Hospital, ShaTin, New Territories, Hong Kong SAR, [5]Department of Medicine, Baylor College of Medicine, Houston, TX 77030, USA

[†] Equal Contribution

* To whom correspondence should be addressed at: Neurologic Research Institute, Suite N.1050, 1250 Moursund Ave, Houston, TX 77030 USA. Tel: +1 8328248716; Fax: +1 8328251240; Email: michael.wangler@bcm.edu

AND Shweta Dhar: One Baylor Plz, MS 228, Baylor College of Medicine, Houston, TX 77030, USA. Tel: +1 7137987764; Fax: +1 7137986450; Email: dhar@bcm.edu

Running Title: DNM1L GTPase effector domain variant in epilepsy

ABSTRACT

DNM1L encodes a GTPase of the dynamin superfamily which plays a crucial role in mitochondrial and peroxisomal fission. Pathogenic variants affecting the middle domain and the GTPase domain of *DNM1L* have been implicated in encephalopathy due to defective mitochondrial and peroxisomal fission 1 (EMPF1, MIM #614388). Patients show variable phenotypes ranging from severe hypotonia leading to death in the neonatal period to developmental delay/regression, with or without seizures. Familial pathogenic variants in the GTPase domain have also been associated with isolated optic atrophy.

We present a 27 year old woman with static encephalopathy, a history of seizures and nystagmus, in whom a novel *de novo* heterozygous variant was detected in the GTPase Effector Domain (GED) of *DNM1L* (c.2072A>G, p.Tyr691Cys). Functional studies in *Drosophila* demonstrate large, abnormally-distributed peroxisomes and mitochondria, an effect very similar to that of middle-domain missense alleles observed in pediatric subjects with EMPF1. To our knowledge, not only is this the first report of a disease-causing variant in the GED domain in humans, but this is also the oldest living individual reported with EMPF1. Longitudinal data of this kind helps to expand our knowledge of the natural history of a growing list of *DNM1L*-related disorders.

INTRODUCTION

DNM1L encodes Dynamin-related Protein 1 (DRP1), an 80kDa GTPase of the dynamin superfamily. Dynamins play crucial roles in vesicle formation and organelle division; specifically, DRP1 plays a crucial role in mitochondrial and peroxisomal fission (division) as well as mitochondrial trafficking and distribution (Otsuga et al. 1998; Pitts et al. 1999; Smirnova et al. 2001; Koch et al. 2003; Wakabayashi et al. 2009). Disruption of mitochondrial dynamics, the balance between mitochondrial fission and fusion, affects mitochondrial integrity (Chan 2012), leading to neuropathy (Zuchner et al. 2004) and neurodegenerative diseases (Beal 2005; Reddy 2009; Burte et al. 2015). DRP1 dysfunction has been implicated in mitochondrial disorders and neurodegenerative disorders including Alzheimer's, Parkinson's and Huntington's disease (Wang et al. 2009; Reddy et al. 2011). Indeed, deletion of neural-specific *Drp1* in mice is lethal shortly after birth, resulting in brain hypoplasia, abnormal neurites and defective synapse formation (Ishihara et al. 2009).

DRP1 is recruited to the outer mitochondrial membrane to interact with receptors such as fission protein 1 (FIS1), mitochondrial fission factor (MFF), mitochondrial dynamics protein of 49 kDa (MID49) and mitochondrial dynamics protein of 51 kDa (MID51) (Chan 2012). In that context, DRP1 acts by forming homodimers which self-assemble into higher-order structures that create a "band" around the mitochondria, which constricts to induce fission (Smirnova et al. 2001). Disruption of this process results in fewer, longer, abnormally distributed mitochondria and peroxisomes (Pitts et al. 1999; Smirnova et al. 2001; Yoon et al. 2001; Koch et al. 2003; Li and Gould 2003). Studies have implicated *DNM1L* variants in impaired mitochondrial function, including impaired mitochondrial fission, reduced membrane potential, and lower oxidative capacity resulting in increased cellular levels of reactive oxygen species (ROS) and double-stranded DNA breaks (Hogarth et al. 2018).

DRP1 is highly homologous to dynamin proteins, sharing the 3 major dynamin domains: the GTPase domain which is conserved, the middle domain and the GTPase effector domain (GED). Pathogenic variants in model systems affecting all 3 domains have been shown to ultimately impact the oligomerization and self-assembly of DRP1 (Ramachandran et al. 2007; Chang et al. 2010; Hogarth et al. 2018). The GTPase domain is also responsible for the conformational change driving the fission process of mitochondria and peroxisomes (Mears et al. 2011). The GED domain stimulates the GTPase activity and participates in formation and stability of the DRP1 homodimer complex (Zhu et al. 2004).

Pathogenic variants in *DNM1L* are associated with a neurological disorder referred to as Encephalopathy due to Defective Mitochondrial and Peroxisomal Fission 1 (EMPF1, OMIM #603850). Affected individuals have variable phenotypes ranging from severe hypotonia leading to death in the neonatal period to developmental delay/regression, with or without seizures. The first patient, described in 2007 (Waterham et al. 2007), was a newborn girl with microcephaly, abnormal brain development, optic atrophy, persistent lactic acidemia and mildly elevated plasma very long chain fatty acids (VLCFA). Immunofluorescent studies of the patient's fibroblasts showed abnormal peroxisomes and mitochondria in a pattern that resembled mammalian cells affected by overexpression of *DNM1L* pathogenic variants or *DNM1L* downregulation (Pitts et al. 1999; Smirnova et al. 2001; Yoon et al. 2001; Koch et al. 2003; Li and Gould 2003). This finding led to identification of a novel heterozygous variant in the middle domain of *DNM1L*. For nearly 10 years no other patients were described but recent studies have dramatically expanded the number of patients and range of phenotypes (Gerber et al. 2018; Wangler et al. 2018a). These studies include reports of heterozygous missense variants in the middle domain of *DNM1L* in nine

unrelated individuals (Chao et al. 2016; Fahrner et al. 2016; Sheffer et al. 2016; Vanstone et al. 2016; Zaha et al. 2016; Diez et al. 2017; Ryan et al. 2018). From model organism studies, the mechanism appears to be dominant negative.

Pathogenic variants in the GTPase domain of *DNM1L* have also been implicated in human disease. Biallelic pathogenic variants (compound heterozygous variants including at least one gene-disrupting allele (Nasca et al. 2016; Yoon et al. 2016) and homozygous missense variants (Hogarth et al. 2018)) in this domain have been associated with a neurological phenotype in 5 patients from 3 unrelated families, whereas heterozygous variants were found to segregate in families with autosomal dominant isolated optic atrophy (Gerber et al. 2017). While the biallelic variants were found to result in loss of function (Nasca et al. 2016; Yoon et al. 2016), functional analysis of the heterozygous variants associated with optic atrophy was suggestive of a restricted dominant negative effect (Gerber et al. 2017; Gerber et al. 2018). To our knowledge, disease-causing variants in the GED domain have never been reported in humans. Here we present a 27 year-old previously undiagnosed female with severe encephalopathy and disability and a history of seizures and nystagmus. Whole exome sequencing (WES) identified a novel variant in the GED domain of *DNM1L*, which we study in *Drosophila*.

RESULTS

Clinical presentation and family history

The patient is a 27 year old female who was evaluated in our Adult Genetics clinic for encephalopathy, disability and epilepsy (**Figure 1A**). She was born to non-consanguineous Caucasian parents (**Figure 1B**). The pregnancy was reportedly normal, with no history of maternal infections or exposures, unremarkable fetal ultrasounds and normal fetal movements. She was delivered at term, with a birth weight of 8 lb 2 oz. At birth, she was noted to have hypotonia, but did not require any special care and did not have significant respiratory or feeding difficulties. She was also noted to have nystagmus, and an ophthalmological exam in infancy revealed optic atrophy although her vision remained intact.

At age 3 months the patient developed unprovoked myoclonic seizures. Workup was unrevealing, and seizures did not recur for several years. The patient had global developmental delay as a child and was later diagnosed with static encephalopathy. She never walked independently, but was able to ambulate using a walker at the age of 3. Over time she developed spasticity and became wheelchair-bound. She has also developed spastic quadriparesis and severe scoliosis requiring surgery in her teens. The patient verbally expressed less than 5 words, but was somewhat able to communicate using a picture communication board. Around 12 years of age, she began to have partial complex seizures, including episodes of status epilepticus, which were refractory to several antiepileptic drugs. At this time, she also developed cyclic vomiting which necessitated hospitalization for rehydration. Repeat EEGs showed background slowing without focal or lateralizing abnormalities and no epileptiform activity. Brain imaging studies including CT and MRI showed some degree of cerebellar atrophy. Seizures were well-controlled at age 20 years with levetiracetam and lamotrigine, and she has remained seizure-free since. The patient has never had behavioral problems and her demeanor has always been pleasant. She requires assistance with activities of daily living, was able to finger-feed herself in the past but has had a general deterioration with reduced energy level in her 20's. Delayed menarche (onset at age 20 years) was also present. On exam at

age 27 years she was non-dysmorphic, visually attentive and had axial hypertonia with diffuse muscle wasting, spasticity and brisk deep tendon reflexes bilaterally with clonus.

Differential diagnoses of mitochondrial disease, chromosomal anomaly, neurotransmitter disorder and *POLG*-related disorders were considered. Extensive metabolic workup over the years including lactate, pyruvate, very long chain fatty acids (VLCFA), plasma amino acids, urine organic acids, acylcarnitine profile, serum creatine/guanidinoacetate and transferrin isoelectric focusing was not informative. CSF analysis revealed a slightly decreased level of tetrahydrobiopterin but normal/slightly increased neurotransmitter levels. In this context, it did not seem likely that her symptoms resulted from a neurotransmitter abnormality, and she had a limited response to a trial of carbidopa-levodopa.

Genomic Analyses

The patient had undergone an extensive prior diagnostic workup since the onset of her symptoms in infancy without any etiologic diagnosis (**Figure 1C**). Previous genetic testing, including array CGH (version 5.0 and Oligo version 8.1.1, Kleberg Cytogenetics Laboratory, Houston, TX), mitochondrial DNA sequencing and single nuclear gene testing (*MECP2*, *CDKL5*, *SCN1A* and *POLG*) was unrevealing. Whole exome sequencing (WES) in 2012 was non-diagnostic, however reanalysis of WES data in 2017 detected a heterozygous, *de novo* novel variant in exon 19 of *DNM1L* (NM_012062, chr12:32895600; c.2072A>G, p.Tyr691Cys). This missense variant had not been previously reported as pathogenic and was absent from the gnomAD and ExAC databases (Lek et al. 2016). The variant substitutes a highly conserved amino acid residue in the GED domain of DRP1, with a combined annotation dependent depletion score (CADD score) of 28.4 (Kircher et al. 2014) (**Figure 2**). In-silico predictions are discordant: "tolerated" by SIFT and "probably damaging" by PolyPhen-2. Though this variant affects the GED domain of the protein and all previous pathogenic *de novo* events were found to affect the middle domain (**Supplementary Table 1**), the variant was classified as "likely pathogenic" by ACMG criteria (Richards et al. 2015). No other variants in known disease-causing genes that may explain the phenotype were reported (**Table 1**).

Metabolic profiling

Given that *DNM1L* is associated with changes in mitochondrial and peroxisomal dynamics, we searched for clinical evidence of mitochondrial or peroxisomal dysfunction. Notably, previously reported *DNM1L* cases have not consistently shown defects in plasma VLCFA nor elevated lactate (**Table 2**). Nevertheless, we sought to find whether the patient has any biochemical abnormalities that indicate perturbations of these functions. We applied global metabolomic profiling through Baylor Genetics Laboratories (Miller et al. 2015; Kennedy et al. 2017) which is a biochemical small-molecule metabolic profile analysis, that was recently utilized to establish a biochemical profile of patients with peroxisomal disorders (Wangler et al. 2018b). Analysis of biochemical analytes from the patient's plasma did not reveal any obvious overlap between the analytes that are characteristically altered in peroxisome biogenesis disorders and the patient's sample (**Supplementary Table 2**). However, the characteristic metabolite changes associated with peroxisomal disorders are known to attenuate with age. Moreover, the patient had previously had normal VLCFA analysis. Therefore, we were unable to functionally validate the pathogenicity of the *DNM1L* variant in the clinic and functional studies in a model organism were needed.

Peroxisomal morphology studies in *Drosophila melanogaster*

To functionally assess the effect of the patient's variant on peroxisomes and mitochondria, we undertook a study in *Drosophila melanogaster*. *Drosophila drp1* is the closest homolog of *DNM1L*. *Drosophila drp1* ($drp1^{1}/drp1^{2}$) mutants are lethal, with impaired mitochondrial trafficking to synapses, mitochondrial morphology and synaptic transmission (Verstreken et al. 2005). Previously, we demonstrated that a middle domain variant of *DNM1L*, p.G350R, identified in a 14 month-old male with global developmental delay and seizures, failed to rescue fly *drp1* mutants. Overexpression of this variant impaired mitochondrial trafficking and altered mitochondrial and peroxisomal morphology (Chao et al. 2016). We engineered the p.Y691C variant found in our patient into a codon-optimized human *DNM1L* construct, and generated transgenic flies carrying the human *DNM1L* gene with and without the patient's variant. We compared the effect of the p.Y691C variant ($DNM1L^{Y691C}$) to that of the p.G350R variant ($DNM1L^{G350R}$) that we previously studied with this system (Chao et al. 2016) (**Figure 3A-B**). In addition, we generated another control construct that deleted the GED domain entirely ($DNM1L^{\Delta GED}$). The $DNM1L^{\Delta GED}$ construct was generated in order to test whether specific deletion of this domain in *Drosophila* also results in lethality or alters peroxisomal morphology.

$DNM1L^{Y691C}$ fails to rescue *Drosophila drp1* mutants

To demonstrate that the human reference sequence construct ($DNM1L^{Ref}$) was able to rescue a *drp1* fly mutant ($drp1^{1}/drp1^{2}$), we crossed the transgenes into *drp1* backgrounds. By expressing human $DNM1L^{Ref}$ ubiquitously with Da-GAL4, we rescued the lethality of *drp1* mutants (**Figure 3A, Supplementary Figure 1, Supplementary Table 3**). As expected, the $DNM1L^{G350R}$ construct from the previously reported case did not rescue lethality. The $DNM1L^{Y691C}$ construct also did not rescue lethality although we did observe some escapers. Interestingly, the $DNM1L^{\Delta GED}$ led to partial rescue with dramatically reduced Mendelian ratios.

Overexpression of $DNM1L^{Y691C}$, but not deletion of the GED domain, results in peroxisomal abnormalities

In order to study the effect of $DNM1L^{Y691C}$ on peroxisomes, the fly transgenic lines were crossed to an Actin-GAL4, UAS-GFP-SKL peroxisomal marker line as previously described (Wangler et al. 2018b). We observed larger peroxisomal size and perinuclear distribution of the peroxisomes in salivary glands of both the $DNM1L^{Y691}$ and $DNM1L^{G350R}$ mutants. Overexpression of the wild type protein did not affect peroxisomal morphology (**Figure 3C-H**). Finally, in order to determine if the effect of the p.Y691C variant was due to loss of the GED domain or a dominant negative effect we over-expressed the $DNM1^{\Delta GED}$ in salivary glands of *Drosophila* larvae. Interestingly these mutants did not exhibit the perinuclear distribution or the large organelle size as in the $DNM1L^{Y691}$ and $DNM1L^{G350R}$ mutants (**Figure 3C-H**), arguing against loss of function as a mechanism for this phenotype. We did test the expression levels in all the different constructs using quantitative PCR. We saw no striking differences, there was a mild relatively higher expression level in the $DNM1L^{Ref}$ compared to the other three constructs (**Supplementary Figure 2, Supplementary Table 4**).

Overexpression of $DNM1L^{Y691C}$ causes mitochondrial morphology aberration

In the lethality rescue assay we had observed mild differences between the $DNM1L^{Y691C}$ and the previously studied $DNM1L^{G350R}$ suggesting our patient's GED domain missense allele might be milder than the middle domain alleles, however the peroxisomal studies showed no difference between these suggesting both alleles had strong dominant-negative impact on peroxisome morphology. We hypothesized that the difference in lethality rescue therefore might be due to a different effect of $DNM1L^{Y691C}$ on mitochondrial

fission. Indeed, a recent report of missense, dominant negative GTPase alleles showed a differential impact on mitochondria without a significant peroxisomal impact (Gerber et al. 2017). *DNM1L* has a well-established impact on mitochondrial fission observed in the middle domain alleles (Chao et al. 2016). We therefore tested mitochondrial morphology in transgenic fly lines of $DNM1L^{Ref}$ versus $DNM1L^{Y691C}$ These were crossed with MEF2-GAL4 in a sensitized genetic background ($drp1^{1}$/+). We noticed a dramatic change in muscle mitochondrial morphology (**Figure 4A-B**) and distribution (**Figure 4C-D**). $DNM1L^{Y691C}$ transgenics displayed a network of mitochondria near the muscle perinuclear region (**Figure 4E**) with a scarcity of mitochondria in muscle fibers as compared with $DNM1L^{Ref}$ (**Figure 4F**). This effect was very similar to the effect of middle domain variants $DNM1L^{G350R}$ and $DNM1L^{A395D}$ we have previously shown (Chao et al. 2016). Therefore, we observed a similar impact of the $DNM1L^{Y691C}$ allele on mitochondria as observed on peroxisomes suggesting a dominant negative allele.

DISCUSSION

Here, we describe an adult patient with a unique phenotype due to a *DNM1L* GED domain *de novo* variant. We use *Drosophila* models to show that this p.Y691C variant fails to rescue *Drosophila drp1* lethality and it results in a strikingly abnormal peroxisomal phenotype, with abnormally-shaped peroxisomes in irregular distribution, likely consistent with a dominant negative effect (**Figure 3C-F**). Our previous studies in *Drosophila* on *DNM1L* also included the p.A395D allele, which had been shown to display dominant negative effects in other assays. Based on this we had confidence in our assay for identifying these effects in this novel mutation. To our knowledge, this is the first report of a pathogenic variant in this domain associated with disease in humans.

Previous reports of pathogenic variants in *DNM1L* associated with a neurological phenotype (EMPF1) include heterozygous variants in the *DNM1L* middle domain with experimentally-confirmed or putative dominant negative effects (Waterham et al. 2007; Chao et al. 2016; Fahrner et al. 2016; Sheffer et al. 2016; Vanstone et al. 2016; Zaha et al. 2016), and biallelic variants (compound heterozygous (Nasca et al. 2016; Yoon et al. 2016) and homozygous (Hogarth et al. 2018) variants) in the GTPase domain with a strong loss of function mechanism. All the biallelic variants reported have been inherited from reportedly unaffected parents, indicating that haploinsufficiency was not a significant factor for these variants (Gerber et al. 2018). Interestingly, heterozygous variants in the GTPase domain result in familial isolated optic atrophy. Results of the functional analysis of these variants also suggest a dominant negative mechanism (Gerber et al. 2017; Gerber et al. 2018). In that case there was a specific effect on mitochondria without a peroxisomal effect. In our study of this GED domain variant, we observe that both organelles are affected. This is consistent with the overall similarity of our patient's clinical phenotypes compared to some of the patients with reported middle domain variants, while the dominant GTPase alleles appear to lead to optic atrophy.

The $DNM1L^{Y691C}$ variant appears to resemble the effect of middle domain variants like $DNM1L^{G350R}$ with respect to both peroxisomal and mitochondrial morphology, although the rescue data suggests it may be a milder allele. Deletion of the GED domain led to a partial loss of function in lethality rescue assays and no dominant negative effect. These data suggest a dominant-negative mechanism for the $DNM1L^{Y691C}$ rather than the loss of GED function. The GED domain plays a role in activation of the GTPase domain. Interestingly, we find that the GED domain is somewhat dispensable (as the truncated protein is still somewhat able to rescue lethality in *drp1* flies). The mechanism by which variants in the GED domain have a dominant negative impact is unclear. One possibility is that the $DNM1L^{Y691C}$ impairs interaction with

other *DNM1L* monomers. Alternatively, the impact could be on the GTPase function indirectly due to the GED associating with the GTPase domain intramolecularly. In support of this, the function of the GED was studied in yeast through investigation of mutant Drp1 harboring a p.K679A mutation (Zhu et al. 2004). The mutant protein had a weaker intramolecular association resulting in impaired GTPase activity, despite unaffected Drp1 complex formation. Interestingly, the amino acid altered in that experiment lies very close to the missense change in our patient (**Figure 2**). Additional structural modeling could clarify this interaction.

The patient we present represents the first report of an adult with a pathogenic *DNM1L* variant resulting in a neurological phenotype. The neurological disorder associated with *DNM1L* is currently termed "EMPF1" and described as a lethal encephalopathy. However, while three cases resulted in death in the neonatal period (Waterham et al. 2007; Yoon et al. 2016) and three other patients died an early death at 18 months (Zaha et al. 2016), 2.5 years (Diez et al. 2017) and 5 years (Chao et al. 2016), other individuals with *DNM1L* pathogenic variants were not critically ill. The majority of the patients presented in the newborn period with hypotonia or later in the first year of life with developmental delay. Two patients had significant developmental regression following apparently normal initial development (Diez et al. 2017; Hogarth et al. 2018). Neurological findings were variable and included spasticity and hyperreflexia, ataxia with pyramidal signs, dystonia and even parkinsonism. Others presented with optic atrophy alone. Our patient (also diagnosed with optic atrophy) presented with neonatal hypotonia progressing to spasticity, developmental delays and static encephalopathy, and survived to adulthood. Her history of transient cyclic vomiting, which is considered a childhood variant of migraine (Rothner 2018), may also be an associated phenotypic feature as altered mitochondrial dynamics and elevated levels of Drp1 have been observed in a rat model of migraine (Dong et al. 2017). Taken together, this highlights the wide spectrum and variability of the neurological phenotypes associated with this disorder (see **Table 2** for the clinical spectrum of *DNM1L*-related disorders and **Supplementary Table 1** for a table of variants).

Given the small number of patients reported to date and the variability of the presentations, genotype-phenotype correlations are difficult to determine. Our patient's attenuated phenotype possibly results from the deleterious effect of the variant on the function of the GED domain, which may differ from the effects of pathogenic variants in the GTPase and middle domains. Some genotype-phenotype correlation for *DNM1L* may be evidenced by the fact that all three patients reported in the literature with the p.R403C variant presented in childhood (ages 4, 5 and 13 years) with acute onset of myoclonus and refractory status epilepticus subsequently leading to brain atrophy and death in one patient, and severe neurological outcome in the others. Two of these patients had some expressive developmental delays prior to the onset of seizures, one of which also had fine motor delays, anxiety and progressive paroxysmal dystonia (Fahrner et al. 2016; Ryan et al. 2018). Out of the 16 reported cases in the literature, 3 occurred in p.R403 and one in p.L406 (a nearby residue), suggesting this may represent a mutational hotspot. Similarly, two distinct alleles have been reported impacting p.G362.

In summary, we describe here a patient with a novel, *de novo* heterozygous variant in the GED domain of the protein encoded by *DNM1L*, which plays an essential role in mitochondrial and peroxisomal dynamics. Functional studies in fly models support a dominant negative mechanism of action for this variant. Given that to date there are no other reports of variants in the GED domain associated with disease in humans, the impact of this domain remains to be explored further. To the best of our knowledge, this is the first report of a *DNM1L* variant in an adult patient with a neurodevelopmental phenotype, expanding the

clinical spectrum of *DNM1L*-related disorders. We conclude that *"DNM1L*-related disorders" comprise a broad range of phenotypes associated with different variations in this gene.

Note Added in Proof

Since the submission of this manuscript three additional reports of DNM1L variants in children with epilepsy and a range of neurological phenotypes have been published (Ladds et al. 2018; Whitley et al. 2018; McCormack et al. 2019).

METHODS

Clinical Cases and Ethics Statement

The patient was enrolled in an IRB-approved human study at Baylor College of Medicine (Houston TX) under the Biochemistry and Cell Biology Correlates of Peroxisomal Disorders (H-32837) and parents provided consented for publication of photos and their clinical data. The clinical workup and sequencing was performed as part of standard clinical care.

Whole Exome Sequencing

The patient underwent clinical whole-exome sequencing through the Baylor Genetics clinical laboratory using standard methods. DNA was isolated from patient's peripheral blood. The next generation sequencing (NGS) library was constructed on covaris sonicator fragmented DNA followed by end repair (NEB, Catalog# E6050L), A-tailing (NEB, Catalog# E6053L) and ligation (Invitrogen, Catalog# A13726101) with Illumina paired end adaptors (unique index sequences) using 1ug of genomic DNA input. The PCR reaction was performed on the samples using the KAPA master mix (KAPA Biosystem, Catalog# KK2612) and primers compatible with Illumina barcode sequences.

The samples were hybridized using Roche NimbleGen developed solution based capture protocol and before incubation index sequencing were blocked by universal blocking Oligos P5 (IDT, Catalog# 1016184) and P7 (IDT, Catalog #1016186). Samples were hybridized using VCRome 2.1 and Spike-in PKv2 probes (lab developed) from 16 hours to 72 hours in a thermocycler at recommended temperature and uncaptured DNA sequenced washed away using Roche hyb wash reagents. The paired end single index run was performed on the Illumina HiSeq 2500 or 2000 platform to obtain average base-pair coverage of >100 with minimal 20X coverage at 95% of targeted sequences (**Supplementary Table 5**). The raw sequencing BCL files were converted to FASTQ file using Illumina CASAVA software version 1.8.3. Raw data were demultiplexed and aligned to human genome reference sequence hg19 and a lab developed software program was used for variant calling and annotation. The variant classification and interpretation were conducted by a clinical standard based on the American College of Medical Genetics and Genomics variant interpretation guidelines.

Exome reanalysis was performed by systematically re-evaluating the variants using updated knowledge base (P.Liu, L.Meng, E.A.Normand, F.Xia, A.Ghazi, J.Rosenfeld, P.L.Magoulas, A.Braxton, P.Ward, H.Dai, B.Yuan, W.Bi, R.Xiao, X.Wang, T.Chiang, F.Vetrini, W.He, H.Cheng, J.Dong, C.Gijavanekar, P.J.Benke, J.A.Bernstein, T.Eble, Y.Eroglu, D.Erwin, L.Escobar, J.B.Gibson, K.Gripp, S.Kleppe, M.K.Koenig, A.M.Lewis,

M.Natowicz, P.Mancias, L.Minor, F.Scaglia, C.Schaaf, H.Streff, H.Vernon, C.L.Uhles, E.H.Zackai, R.Sutton, A.L.Beaudet, D.Muzny, R.A.Gibbs, J.E.Posey, S.Lalani, C.Shaw, C.M.Eng, J.R.Lupski and Y.Yang, manuscript in preparation). Candidate variants were PCR amplified and Sanger sequenced with both the proband and the parental samples.

Metabolic profile analysis

Metabolomic profiling was performed by Baylor Genetics Laboratories (Houston, TX) and Metabolon, Inc (Morrisville, NC), as described previously (Evans et al. 2009; Evans et al. 2014; Miller et al. 2015; Kennedy et al. 2017). Metabolites were identified by matching the ion chromatographic retention index, accurate mass, and mass spectral fragmentation signatures with a reference library consisting of over 4,000 entries from standard metabolites (Dehaven et al. 2010). Metabolite z-scores were generated using the method previously described (Miller et al. 2015; Donti et al. 2016).

***Drosophila* transgenics**

We had previously generated transgenic flies with human *DNM1L* Reference and a p.G350R variant (Chao et al. 2016) ($DNM1L^{Ref}$ and $DNM1L^{G350R}$, respectively). We produced human *DNM1L* p.Y691C variant ($DNM1L^{Y691C}$) and a GED domain deletion construct ($GED^{\Delta GED}$) which were codon-optimized for *Drosophila* expression (GeneArt™). These constructs were subcloned into the pUAST-attB vector. Transgenic flies were produced by injecting prepared DNA into VK00033 embryos (Bischof et al. 2007) and the site for site-specific integration was (y[1] w[1118]; PBac[y[+]-attP-3B]VK00033) (Venken et al. 2006).

***Drosophila* genetics**

The $drp1^{1}$ and $drp1^{2}$ alleles used in this study were reported by Verstreken et.al. (Verstreken et al. 2005). Transgenic *DNM1L* flies were obtained by crossing into these genetic backgrounds.

Peroxisomal morphology studies

Two peroxisomal reporters were used in third instar larval salivary gland, a UAS-GFP-SKL construct generated by subcloning a c-terminal SKL tagged GFP into the UAS vector and a transgenic insertion on second chromosome was recombined with Actin-GAL4 (y1 w*; P{Act5C-GAL4}25FO1/CyO, y+) (Wangler et al. 2017). Pex3 staining was performed as described (Faust et al. 2014). Confocal images were quantified using ImageJ software

Mitochondrial morphology studies

Transgenic flies with UAS-$DNM1L^{Ref}$ or UAS-$DNM1L^{Y691C}$ constructs were crossed with MEF2-GAL4 in a $drp1^{1}$ mutant background. Third instar larval muscles were fixed, permeablilized and stained with primary mouse anti-complex V antibody (abcam 14748) which was then incubated with secondary anti-mouse-Alexa 488 antibody. The muscles were also stained with anti-phalloidin conjugated with Alexa 546 and DAPI. Images were captured for ventral longitudinal muscle 6 and 7 from segment A3 using confocal microscope (Zeiss LSM 880). Image analysis was done using ImageJ software.

mRNA expression analysis

Reverse transcriptase-quantitative PCR (RT-qPCR) was carried out on all the four *DNM1L* flies to asses relative mRNA expression levels among the four genotypic flies. Two biological replicates of 30 adult fly heads were sampled per genotype. Total RNA was isolated from head portions of third instar larvae which

contained salivary glands. Total RNA was extracted from each biological replicate using Triazol RNA isolation. Reverse transcription of total RNA to get cDNA was done using iScript™ Reverse Transcription Supermix for RT-qPCR (Bio-Rad Laboratories, Inc., Hercules, CA) according to the manufacturer's instructions. Equal quantities of this cDNA from each genotype were used to set RT-qPCR reactions for corresponding putative target mRNA transcripts using iQ™ SYBR® Green Supermix (2X) (Bio-Rad Laboratories, Hercules, CA). All amplification reactions were performed in Bio Rad CFX96 Real-Time PCR Machine (Bio-Rad Laboratories, Inc.) with three technical replicates across all biological replicates. Normalized mRNA expression levels were calculated using the $2^{-\Delta\Delta C(t)}$ method (Schmittgen and Livak 2008) with the internal reference as Rpl32.

ADDITIONAL INFORMATION

Data Deposition and Access

All the relevant data are included in the manuscript and supplemental materials, the *DNM1L* variant has been submitted to ClinVar and can be found under accession number SCV000882867. Patient consent for deposition of raw sequencing data was not obtained.

Ethics Statement

The patient was enrolled in an IRB-approved human study at Baylor College of Medicine (Houston TX) under the Biochemistry and Cell Biology Correlates of Peroxisomal Disorders (H-32837) and consented for publication of photos and their clinical data.

Acknowledgements

The authors would like to thank the family for participating in the study. We thank Yu-Hsin Chao for technical support in the design of the *DNM1L* constructs used in this study. We thank Jonathan Andrews for technical advice in the expression analysis.

Author Contributions

NAB- Conceptual design, clinical evaluation, wrote the manuscript
PB- conducted fly experiments
TE- Clinical evaluation
PL- Genomic analysis
CE- Genomic analysis
SE- Metabolomic analysis
LR- conceptual design
FS- conceptual design
AG- cinical evaluation
SD-conceptual design, clinical evaluation
MW- conceptual design, conducted fly experiments, wrote the manuscript

Conflict of Interest:

- Fernando Scaglia receives research support from BioElectron Technologies, Reata Pharmaceuticals and Stealth BioTherapeutics.

REFERENCES

Beal MF. 2005. Mitochondria take center stage in aging and neurodegeneration. *Ann Neurol* **58**: 495-505.

Bischof J, Maeda RK, Hediger M, Karch F, Basler K. 2007. An optimized transgenesis system for Drosophila using germ-line-specific phiC31 integrases. *Proc Natl Acad Sci U S A* **104**: 3312-3317.

Burte F, Carelli V, Chinnery PF, Yu-Wai-Man P. 2015. Disturbed mitochondrial dynamics and neurodegenerative disorders. *Nat Rev Neurol* **11**: 11-24.

Chan DC. 2012. Fusion and fission: interlinked processes critical for mitochondrial health. *Annu Rev Genet* **46**: 265-287.

Chang CR, Manlandro CM, Arnoult D, Stadler J, Posey AE, Hill RB, Blackstone C. 2010. A lethal de novo mutation in the middle domain of the dynamin-related GTPase Drp1 impairs higher order assembly and mitochondrial division. *J Biol Chem* **285**: 32494-32503.

Chao YH, Robak LA, Xia F, Koenig MK, Adesina A, Bacino CA, Scaglia F, Bellen HJ, Wangler MF. 2016. Missense variants in the middle domain of DNM1L in cases of infantile encephalopathy alter peroxisomes and mitochondria when assayed in Drosophila. *Hum Mol Genet* **25**: 1846-1856.

Dehaven CD, Evans AM, Dai H, Lawton KA. 2010. Organization of GC/MS and LC/MS metabolomics data into chemical libraries. *J Cheminform* **2**: 9.

Diez H, Cortes-Saladelafont E, Ormazabal A, Marmiese AF, Armstrong J, Matalonga L, Bravo M, Briones P, Emperador S, Montoya J et al. 2017. Severe infantile parkinsonism because of a de novo mutation on DLP1 mitochondrial-peroxisomal protein. *Mov Disord* **32**: 1108-1110.

Dong X, Guan X, Chen K, Jin S, Wang C, Yan L, Shi Z, Zhang X, Chen L, Wan Q. 2017. Abnormal mitochondrial dynamics and impaired mitochondrial biogenesis in trigeminal ganglion neurons in a rat model of migraine. *Neurosci Lett* **636**: 127-133.

Donti TR, Cappuccio G, Hubert L, Neira J, Atwal PS, Miller MJ, Cardon AL, Sutton VR, Porter BE, Baumer FM et al. 2016. Diagnosis of adenylosuccinate lyase deficiency by metabolomic profiling in plasma reveals a phenotypic spectrum. *Mol Genet Metab Rep* **8**: 61-66.

Evans AM, Bridgewater BR, Liu Q, Mitchell MW, Robinson RJ, Dai H, Stewart SJ, DeHaven CD, Miller LAD. 2014. High Resolution Mass Spectrometry Improves Data Quantity and Quality as Compared to Unit Mass Resolution Mass Spectrometry in High-Throughput Profiling Metabolomics. *Metabolomics* **4**.

Evans AM, DeHaven CD, Barrett T, Mitchell M, Milgram E. 2009. Integrated, nontargeted ultrahigh performance liquid chromatography/electrospray ionization tandem mass spectrometry platform for the identification and relative quantification of the small-molecule complement of biological systems. *Anal Chem* **81**: 6656-6667.

Fahrner JA, Liu R, Perry MS, Klein J, Chan DC. 2016. A novel de novo dominant negative mutation in DNM1L impairs mitochondrial fission and presents as childhood epileptic encephalopathy. *Am J Med Genet A* **170**: 2002-2011.

Faust JE, Manisundaram A, Ivanova PT, Milne SB, Summerville JB, Brown HA, Wangler M, Stern M, McNew JA. 2014. Peroxisomes are required for lipid metabolism and muscle function in Drosophila melanogaster. *PLoS One* **9**: e100213.

Gerber S, Charif M, Chevrollier A, Chaumette T, Angebault C, Kane MS, Paris A, Alban J, Quiles M, Delettre C et al. 2017. Mutations in DNM1L, as in OPA1, result indominant optic atrophy despite opposite effectson mitochondrial fusion and fission. *Brain* **140**: 2586-2596.

Gerber S, Charif M, Chevrollier A, Chaumette T, Angebault C, Kane S, Paris A, Alban J, Quiles M, Delettre C et al. 2018. Reply: The expanding neurological phenotype of DNM1L-related disorders. *Brain* **141**: e29.

Hogarth KA, Costford SR, Yoon G, Sondheimer N, Maynes JT. 2018. DNM1L Variant Alters Baseline Mitochondrial Function and Response to Stress in a Patient with Severe Neurological Dysfunction. *Biochem Genet* **56**: 56-77.

Ishihara N, Nomura M, Jofuku A, Kato H, Suzuki SO, Masuda K, Otera H, Nakanishi Y, Nonaka I, Goto Y et al. 2009. Mitochondrial fission factor Drp1 is essential for embryonic development and synapse formation in mice. *Nat Cell Biol* **11**: 958-966.

Kennedy AD, Pappan KL, Donti TR, Evans AM, Wulff JE, Miller LAD, Reid Sutton V, Sun Q, Miller MJ, Elsea SH. 2017. Elucidation of the complex metabolic profile of cerebrospinal fluid using an untargeted biochemical profiling assay. *Mol Genet Metab* **121**: 83-90.

Kircher M, Witten DM, Jain P, O'Roak BJ, Cooper GM, Shendure J. 2014. A general framework for estimating the relative pathogenicity of human genetic variants. *Nat Genet* **46**: 310-315.

Koch A, Thiemann M, Grabenbauer M, Yoon Y, McNiven MA, Schrader M. 2003. Dynamin-like protein 1 is involved in peroxisomal fission. *J Biol Chem* **278**: 8597-8605.

Ladds E, Whitney A, Dombi E, Hofer M, Anand G, Harrison V, Fratter C, Carver J, Barbosa IA, Simpson M et al. 2018. De novo DNM1L mutation associated with mitochondrial epilepsy syndrome with fever sensitivity. *Neurol Genet* **4**: e258.

Lek M, Karczewski KJ, Minikel EV, Samocha KE, Banks E, Fennell T, O'Donnell-Luria AH, Ware JS, Hill AJ, Cummings BB et al. 2016. Analysis of protein-coding genetic variation in 60,706 humans. *Nature* **536**: 285-291.

Li X, Gould SJ. 2003. The dynamin-like GTPase DLP1 is essential for peroxisome division and is recruited to peroxisomes in part by PEX11. *J Biol Chem* **278**: 17012-17020.

McCormack M, McGinty R, Zhu X, Slattery L, Heinzen EL, Consortium E, Costello DJ, Delanty N, Cavalleri GL. 2019. De-novo mutations in patients with chronic ultra-refractory epilepsy with onset after age five years. *Eur J Med Genet* doi:10.1016/j.ejmg.2019.01.015.

Mears JA, Lackner LL, Fang S, Ingerman E, Nunnari J, Hinshaw JE. 2011. Conformational changes in Dnm1 support a contractile mechanism for mitochondrial fission. *Nat Struct Mol Biol* **18**: 20-26.

Miller MJ, Kennedy AD, Eckhart AD, Burrage LC, Wulff JE, Miller LA, Milburn MV, Ryals JA, Beaudet AL, Sun Q et al. 2015. Untargeted metabolomic analysis for the clinical screening of inborn errors of metabolism. *J Inherit Metab Dis* **38**: 1029-1039.

Nasca A, Legati A, Baruffini E, Nolli C, Moroni I, Ardissone A, Goffrini P, Ghezzi D. 2016. Biallelic Mutations in DNM1L are Associated with a Slowly Progressive Infantile Encephalopathy. *Hum Mutat* **37**: 898-903.

Otsuga D, Keegan BR, Brisch E, Thatcher JW, Hermann GJ, Bleazard W, Shaw JM. 1998. The dynamin-related GTPase, Dnm1p, controls mitochondrial morphology in yeast. *J Cell Biol* **143**: 333-349.

Pitts KR, Yoon Y, Krueger EW, McNiven MA. 1999. The dynamin-like protein DLP1 is essential for normal distribution and morphology of the endoplasmic reticulum and mitochondria in mammalian cells. *Mol Biol Cell* **10**: 4403-4417.

Ramachandran R, Surka M, Chappie JS, Fowler DM, Foss TR, Song BD, Schmid SL. 2007. The dynamin middle domain is critical for tetramerization and higher-order self-assembly. *EMBO J* **26**: 559-566.

Reddy PH. 2009. Amyloid beta, mitochondrial structural and functional dynamics in Alzheimer's disease. *Exp Neurol* **218**: 286-292.

Reddy PH, Reddy TP, Manczak M, Calkins MJ, Shirendeb U, Mao P. 2011. Dynamin-related protein 1 and mitochondrial fragmentation in neurodegenerative diseases. *Brain Res Rev* **67**: 103-118.

Richards S, Aziz N, Bale S, Bick D, Das S, Gastier-Foster J, Grody WW, Hegde M, Lyon E, Spector E et al. 2015. Standards and guidelines for the interpretation of sequence variants: a joint consensus recommendation of the American College of Medical Genetics and Genomics and the Association for Molecular Pathology. *Genet Med* **17**: 405-424.

Rothner AD. 2018. Migraine Variants in Children. *Pediatr Ann* **47**: e50-e54.

Ryan CS, Fine AL, Cohen AL, Schiltz BM, Renaud DL, Wirrell EC, Patterson MC, Boczek NJ, Liu R, Babovic-Vuksanovic D et al. 2018. De Novo DNM1L Variant in a Teenager With Progressive Paroxysmal Dystonia and Lethal Super-refractory Myoclonic Status Epilepticus. *J Child Neurol* doi:10.1177/0883073818778203: 883073818778203.

Schmittgen TD, Livak KJ. 2008. Analyzing real-time PCR data by the comparative C(T) method. *Nat Protoc* **3**: 1101-1108.

Sheffer R, Douiev L, Edvardson S, Shaag A, Tamimi K, Soiferman D, Meiner V, Saada A. 2016. Postnatal microcephaly and pain insensitivity due to a de novo heterozygous DNM1L mutation causing impaired mitochondrial fission and function. *Am J Med Genet A* **170**: 1603-1607.

Smirnova E, Griparic L, Shurland DL, van der Bliek AM. 2001. Dynamin-related protein Drp1 is required for mitochondrial division in mammalian cells. *Mol Biol Cell* **12**: 2245-2256.

Vanstone JR, Smith AM, McBride S, Naas T, Holcik M, Antoun G, Harper ME, Michaud J, Sell E, Chakraborty P et al. 2016. DNM1L-related mitochondrial fission defect presenting as refractory epilepsy. *Eur J Hum Genet* **24**: 1084-1088.

Venken KJ, He Y, Hoskins RA, Bellen HJ. 2006. P[acman]: a BAC transgenic platform for targeted insertion of large DNA fragments in D. melanogaster. *Science* **314**: 1747-1751.

Verstreken P, Ly CV, Venken KJ, Koh TW, Zhou Y, Bellen HJ. 2005. Synaptic mitochondria are critical for mobilization of reserve pool vesicles at Drosophila neuromuscular junctions. *Neuron* **47**: 365-378.

Wakabayashi J, Zhang Z, Wakabayashi N, Tamura Y, Fukaya M, Kensler TW, Iijima M, Sesaki H. 2009. The dynamin-related GTPase Drp1 is required for embryonic and brain development in mice. *J Cell Biol* **186**: 805-816.

Wang H, Lim PJ, Karbowski M, Monteiro MJ. 2009. Effects of overexpression of huntingtin proteins on mitochondrial integrity. *Hum Mol Genet* **18**: 737-752.

Wangler MF, Assia Batzir N, Robak LA, Koenig MK, Bacino CA, Scaglia F, Bellen HJ. 2018a. The expanding neurological phenotype of DNM1L-related disorders. *Brain* **141**: e28.

Wangler MF, Chao YH, Bayat V, Giagtzoglou N, Shinde AB, Putluri N, Coarfa C, Donti T, Graham BH, Faust JE et al. 2017. Peroxisomal biogenesis is genetically and biochemically linked to carbohydrate metabolism in Drosophila and mouse. *PLoS Genet* **13**: e1006825.

Wangler MF, Hubert L, Donti TR, Ventura MJ, Miller MJ, Braverman N, Gawron K, Bose M, Moser AB, Jones RO et al. 2018b. A metabolomic map of Zellweger spectrum disorders reveals novel disease biomarkers. *Genet Med* doi:10.1038/gim.2017.262.

Waterham HR, Koster J, van Roermund CW, Mooyer PA, Wanders RJ, Leonard JV. 2007. A lethal defect of mitochondrial and peroxisomal fission. *N Engl J Med* **356**: 1736-1741.

Whitley BN, Lam C, Cui H, Haude K, Bai R, Escobar L, Hamilton A, Brady L, Tarnopolsky MA, Dengle L et al. 2018. Aberrant Drp1-mediated mitochondrial division presents in humans with variable outcomes. *Hum Mol Genet* **27**: 3710-3719.

Yoon G, Malam Z, Paton T, Marshall CR, Hyatt E, Ivakine Z, Scherer SW, Lee KS, Hawkins C, Cohn RD et al. 2016. Lethal Disorder of Mitochondrial Fission Caused by Mutations in DNM1L. *J Pediatr* **171**: 313-316 e311-312.

Yoon Y, Pitts KR, McNiven MA. 2001. Mammalian dynamin-like protein DLP1 tubulates membranes. *Mol Biol Cell* **12**: 2894-2905.

Zaha K, Matsumoto H, Itoh M, Saitsu H, Kato K, Kato M, Ogata S, Murayama K, Kishita Y, Mizuno Y et al. 2016. DNM1L-related encephalopathy in infancy with Leigh syndrome-like phenotype and suppression-burst. *Clin Genet* **90**: 472-474.

Zhu PP, Patterson A, Stadler J, Seeburg DP, Sheng M, Blackstone C. 2004. Intra- and intermolecular domain interactions of the C-terminal GTPase effector domain of the multimeric dynamin-like GTPase Drp1. *J Biol Chem* **279**: 35967-35974.

Zuchner S, Mersiyanova IV, Muglia M, Bissar-Tadmouri N, Rochelle J, Dadali EL, Zappia M, Nelis E, Patitucci A, Senderek J et al. 2004. Mutations in the mitochondrial GTPase mitofusin 2 cause Charcot-Marie-Tooth neuropathy type 2A. *Nat Genet* **36**: 449-451.

Figure Legends

Figure 1 – **A.** The patient at age 27 years. She is non-verbal non-ambulatory but is able to partially communicate using a communication board. **B.** Patient's pedigree. **C.** Timeline of clinical symptoms and diagnostic testing. Time is shown on the X-axis. Clinical symptoms are depicted above the timeline corresponding to time of onset. Duration of symptoms occurring over a period of time is indicated with blue boxes. Below the line, diagnostic studies are shown with red arrowheads indicating time of studies. VLCFA – very-long-chain fatty acids. PAA – plasma amino acids. UOA –urine organic acids. ACP – acylcarnitine profile. CSF – cerebrospinal fluid. Array CGH v5.0 indicates Array Comparative Genomic Hybridization version 5.0. Array CGH v8.1.1 indicates Array Comparative Genomic Hybridization version 8.1.1 (Baylor Genetics). WES – Whole Exome Sequencing (Baylor Genetics).

Figure 2 – *DNM1L* alleles associated with human disease. **A.** The *DNM1L* gene encoding the DRP1 protein is shown in schematic. Each mutation is shown at its position on the encoded protein. Shaded arrowheads indicate the zygosity and associated phenotype as seen on the legend. Red: heterozygous variants associated with an autosomal dominant neurological disorder. Dark blue: compound heterozygous or homozygous variants associated with an autosomal recessive neurological disorder. Light Blue: heterozygous variants associated with dominant isolated optic atrophy. The red arrow indicates the patient's variant (p.Y691C). EMPF1 - Encephalopathy, lethal, due to defective mitochondrial peroxisomal fission 1. **B.** Sequence alignment of the amino acid stretch surrounding the $DNM1L^{Y691C}$ in DNM1L (H. sapiens), ADL2b (A. thaliana), Vps1p (S. cerevisiae) and DymA (D. discoideum). Residues conserved among all 4 species are shaded in yellow. Residues identical in 3 out of 4 species are shaded in blue. GenBankTM accession numbers: DNM1L,BAA22193; ADL2b, BAB85645; Vps1p, NP_012926; and DymA, CAA67983. Position of the last amino acid in the alignment is indicated. The Y691C variant alters a conserved residue in the GED domain (red arrow). A point mutation in a nearby conserved residue (p.K679A, marked by asterisk) was previously shown to alter the intramolecular association between the GED domain and GTPase domain (Zhu et al. 2004).

Figure 3 – Functional studies in *Drosophila melanogaster*. **A.** Table of rescue crosses showing lethality rescue results for *drp1* mutants expressing the constructs shown. **B.** Schematic of the constructs and the location of the mutations in the *DNM1L* domains. **C-F.** Dominant effects of DNM1L expression on *Drosophila* salivary gland peroxisomes. **(C-C")** *Drosophila* salivary gland cells are shown with expression of the reference *DNM1L* with Actin-GAL4 alongside UAS-EGFP-SKL (Chao et al. 2016) and co-stained with *Drosophila* anti-Pex3 antibody. **(D-D")** Middle domain variant p.G350R (Chao et al. 2016) produces enlarged peroxisomes with abnormal distribution. Fewer peroxisomes are apparent in the cell. **(E-E")** GED domain variant p.Y691C (seen in Patient) produces enlarged peroxisomes with abnormal distribution and fewer peroxisomes are apparent in the cell similar to p.G350R. **(F-F")** $DNM1L^{\Delta GED}$ construct does not appear to have a dramatic effect on peroxisomal size as well as number of peroxisomes per sample as compared with $DNM1L^{Ref}$. **(G)** Quantification of the peroxisomal area per peroxisome (μm2) **(H)** Quantification of number of peroxisomes per sample.

Figure 4 – Functional studies in *Drosophila melanogaster* third instar larval muscle fibers. **A.** A perinuclear section of a muscle fiber from the UAS-$DNM1L^{Ref}$ crossed to MEF2-GAL4 in a sensitized

genetic background (*drp1*^{1}/+). stained with anti-complex V antibody showing a pattern of normal mitochondrial morphology. **A'.** inset of A. **B.** A perinuclear section of a muscle fiber from the UAS-*DNM1L*^{Y691C} stained with anti-complex V antibody crossed to MEF2-GAL4 showing an abnormal interconnected mass of mitochondrial staining without clear delineating between individual organelles. **B'.** inset of B. **C.** A deep muscle fiber section stained with phalloidin and anti-complex V of from the UAS-*DNM1L*^{Ref} crossed to MEF2-GAL4 showing a normal distribution of mitochondria between the sarcomeres. **C'** The same section as C without phalloidin staining shown. **D.** A deep muscle fiber section stained with phalloidin and anti-complex V of from the UAS-*DNM1L*^{Y691C} crossed to MEF2-GAL4 showing a paucity of mitochondria between the sarcomeres. **D'** The same section as D without phalloidin staining shown. **E.** Quantification of numbers of separate mitochondria per micrometer from the perinuclear region, 5 animals per genotype were quantified. **F.** Quantification of the number of mitochondria per sarcomere in deep fiber sections, 5 animals per genotype were quantified.

Table **1:** Likely Pathogenic and Variants of Unknown Significance detected on the patient's whole exome sequencing.

Gene	Chromosome	HGVS DNA Reference	HGVS Protein Reference	Variant Type	Predicted Effect	dbSNP/dbVar ID	Genotype	Parent of Origin
DNM1L	12	NM_012062:c.2072A>G	p.Tyr691Cys	Missense	Substitution	N/A	Het	*De novo*
PPT1	1	NM_000310:c.635A>G	p.Asn212Ser	Missense	Substitution	rs568730410	Het	Maternal
ADCK3	1	NM_020247:c.730G>C	p.Gly244Arg	Missense	Substitution	rs199619932	Het	Maternal
NDUFB3	2	NM_002491:c.19C>T	p.His7Tyr	Missense	Substitution	rs144513268	Het	Paternal
SERPINA1	14	NM_000295:c.1096G>A	p.Glu366Lys	Missense	Substitution	rs28929474	Het	Paternal

AR – autosomal recessive. Het – heterozygous. N/A – not applicable.

Table 2. Clinical spectrum of *DNM1L*-related disorders.

	GTPase Domain						Middle Domain										GED Domain
Publication	**Gerber et al. 2017**	**Nasca et al. 2016**		**Yoon et al. 2016**		**Hogarth et al. 2017**	**Gerber et al. 2017**	**Chao et al. 2016**	**Vanstone et al. 2016**	**Sheffer et al. 2016**	**Waterham et al. 2007**	**Fahrner et al. 2016**		**Ryan et al. 2018**	**Zaha et al. 2016**	**Diez et al. 2017**	**Proband**
Protein change	**Glu2Ala**	**Ser36Gly/ Glu116LysfsTer6**		**Trp88MetfsTer9/ Glu129LysfsTer6**		**Thr115Met**	**Ala192Glu**	**Gly350Arg**	**Gly362Asp**	**Gly362Ser**	**Ala395Asp**	**Arg403Cys**		**Arg403Cys**	**Leu406Ser**	**Cys446Phe**	**Tyr691Cys**
Onset	<10 yrs	1 yr	1 yr	Birth	Birth	1st mos of life	NR	5 mos	<6 mos	<6 mos	6 days	4 yrs	5 yrs	<18 mos	6 mos	3 mos	Birth
Hypotonia	NR	-	-	+++	+++	+	NR	+	Head control at 18 mos	+	+++	-	-	NR	+++	-	+
Dev. delay	-	+	+	N/A	N/A	+	-	+	+	+	+	+	+	+	+	+	+
Dev. regression	-	-	-	N/A	N/A	+	-	+	-	-	N/A	+	+	+ Progressive dystonia	-	+	+
Seizures	-	-	-	-	-	NR	-	+SE	+ SE	-	-	+ SE	+ SE	+SE	+ IS	Tremor, HRS	+ SE
Optic atrophy	+	-	NR	-	-	NR	+	-	NR	-	+	NR	NR	-	NR	NR	+
Nystagmus	NR	Strabismus	Strabismus	NR	NR	NR	NR	+	NR	NR	+	NR	NR	NR	+	OGC	+
Abnormal MRI	-	-	NR	-	HI	+	-	+	-	+	+	+	+	+	+	+	-
Increased lactate	NR	+	-	On MRS	NR	Intermittent	NR	+	-	+	+	-	On MRS	On MRS	+	+	-
Abnormal VLCFA	NR	-	-	-	NR	-	NR	-	-	-	+	-	-	-	NR	NR	-
Mito. abnorm.	+	+	+	+	+	+	+	+	+	+	+	+	+	+	+	+	NR
Peroxi. abnorm.	-	+	+	NR	NR	-	-	+	NR	-	+	NR	NR	NR	+	+	+
Survival	Adult	>16 yrs	>3 yrs	3 weeks	8 days	>4 yrs	Adult	5 yrs	>7 yrs	>2 yrs	37 days	>8 yrs	>7 yrs	13 yrs	18 mos	2.5 yrs	Adult

CSF – cerebrospinal fluid. HI – Hypoxic-ischemic insult. HRS – Hypokinetic-Rigid Syndrome. IS – infantile spasms. Mito. abnorm. – mitochondrial abnormalities (defined as abnormal shape, distribution or functional abnormalities in patients or model systems). Mos – months. MRS – magnetic resonance spectroscopy. N/A – not applicable. NR – not reported. OGC – oculogyric crisis. Peroxi. abnorm. – peroxisomal abnormalities (defined as abnormal shape, distribution or functional abnormalities in patients or model systems). SE – status epilepticus. Yr – year. Yrs – years. +++ indicates severe phenotype.

Abbrevitations

ACP – acylcarnitine profile

Array CGH – Comparative genomic hybridization array

CADD score - Combined annotation dependent depletion score

CSF – Cerebrospinal Fluids

CT – Computed tomography

DNM1L – Dynamin 1-like

DRP1 – Dynamin-related protein 1

EEG - Electroencephalography

EMPF1 - Encephalopathy due to defective mitochondrial and peroxisomal fission 1

GED – GTPase effector domain

MRI – Magnetic resonance imaging

PAA – Plasma amino acids

ROS – Reactive oxygen species

UOA – Urine organic acids

VLCFA – Very long chain fatty acids


A
B
DNM1L:
+/+
DNM1L:
+/+
DNM1L:
p.Y691C/+
C
Clinical symptoms
Diagnostic workup
Developmental delay, static encephalopathy
GTC and partial complex seizures
Myoclonic seizures
Nystagmus
Cyclic vomiting
Scoliosis surgery
Menarche
3 months
12 years
16 years
20 years
27 years
Lactate, pyruvate, VLCFA, PAA, UOA, ACP, serum creatine/guanidinoacetate, transferrin isoelectric focusing, CSF analysis
Karyotype
MECP2
CDKL5
SCN1A
Array CGH V.8.1.1
POLG
WES reanalysis
Mitochondrial DNA Array CGH V.5.0
WES

FIGURE 1

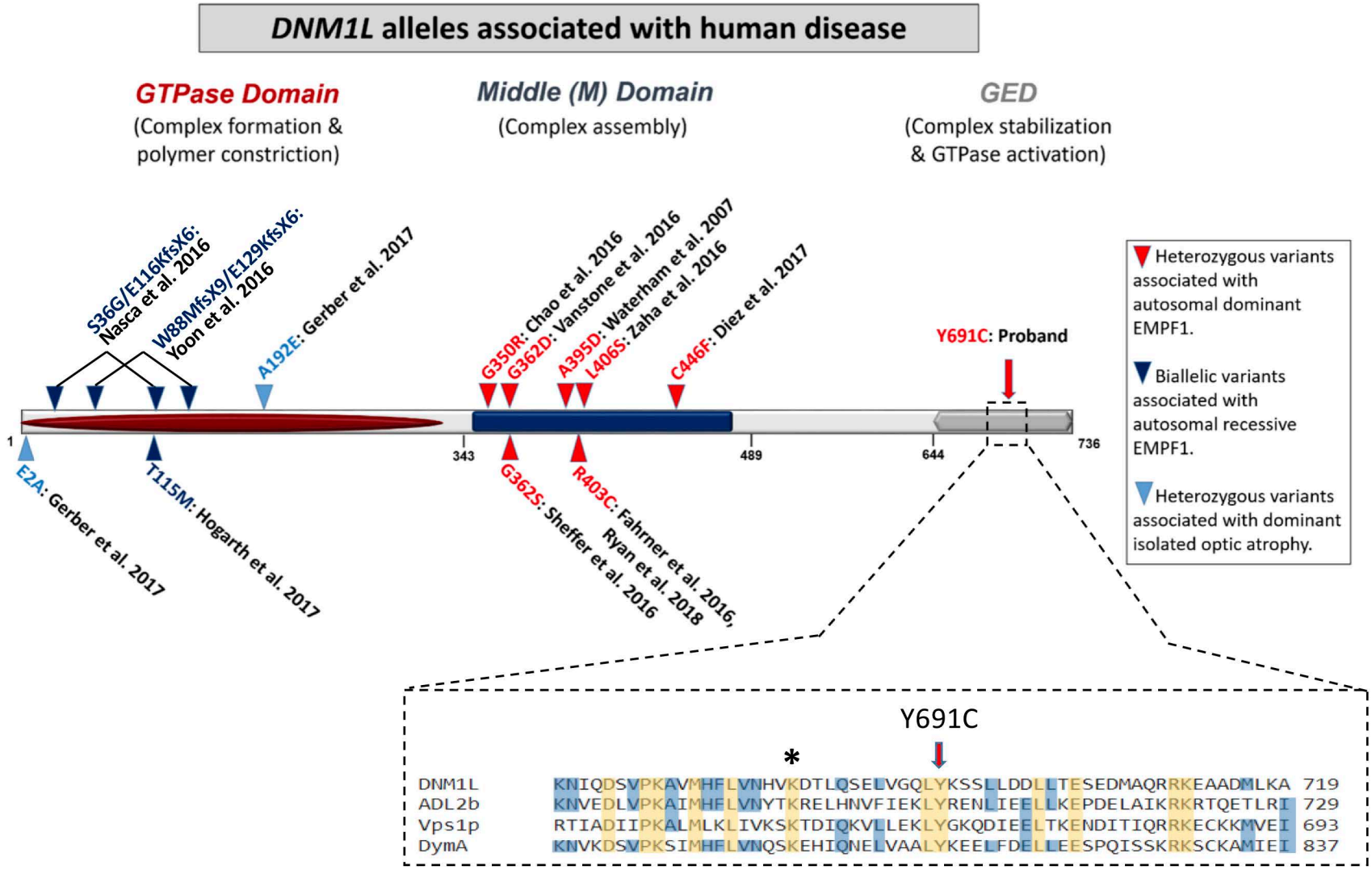
DNM1L alleles associated with human disease
GTPase Domain
(Complex formation & polymer constriction)
Middle (M) Domain
(Complex assembly)
GED
(Complex stabilization & GTPase activation)
S36G/E116KfsX6: Nasca et al. 2016
W88MfsX9/E129KfsX6: Yoon et al. 2016
A192E: Gerber et al. 2017
G350R: Chao et al. 2016
G362D: Vanstone et al. 2016
A395D: Waterham et al. 2007
L406S: Zaha et al. 2016
C446F: Diez et al. 2017
Y691C: Proband
1
343
489
644
736
E2A: Gerber et al. 2017
T115M: Hogarth et al. 2017
G362S: Sheffer et al. 2016
R403C: Fahrner et al. 2016, Ryan et al. 2018
Heterozygous variants associated with autosomal dominant EMPF1.
Biallelic variants associated with autosomal recessive EMPF1.
Heterozygous variants associated with dominant isolated optic atrophy.
Y691C
*
DNM1L KNIQDSVPKAVMHFLVNHVKDTLQSELVGQLYKSSLLDDLLTESEDMAQRRKEAADMLKA 719
ADL2b KNVEDLVPKAIMHFLVNYTKRELHNVFIEKLYRENLIEELLKEPDELAIKRKRTQETLRI 729
Vps1p RTIADIIPKALMLKLIVKSKTDIQKVLLEKLYGKQDIEELTKENDITIQRRKECKKMVEI 693
DymA KNVKDSVPKSIMHFLVNQSKEHIQNELVAALYKEELFDELLEESPQISSKRKSCKAMIEI 837

FIGURE 2

A

	UAS-drp1	*UAS-DNM1L$^{(REF)}$*	*UAS-DNM1L$^{(G350R)}$*	*UAS-DNM1L$^{(Y691C)}$*	*UAS-DNM1L$^{(\Delta GED)}$*
Rescue of drp1 mutant	Yes	Yes	No	Few escapers	Partial

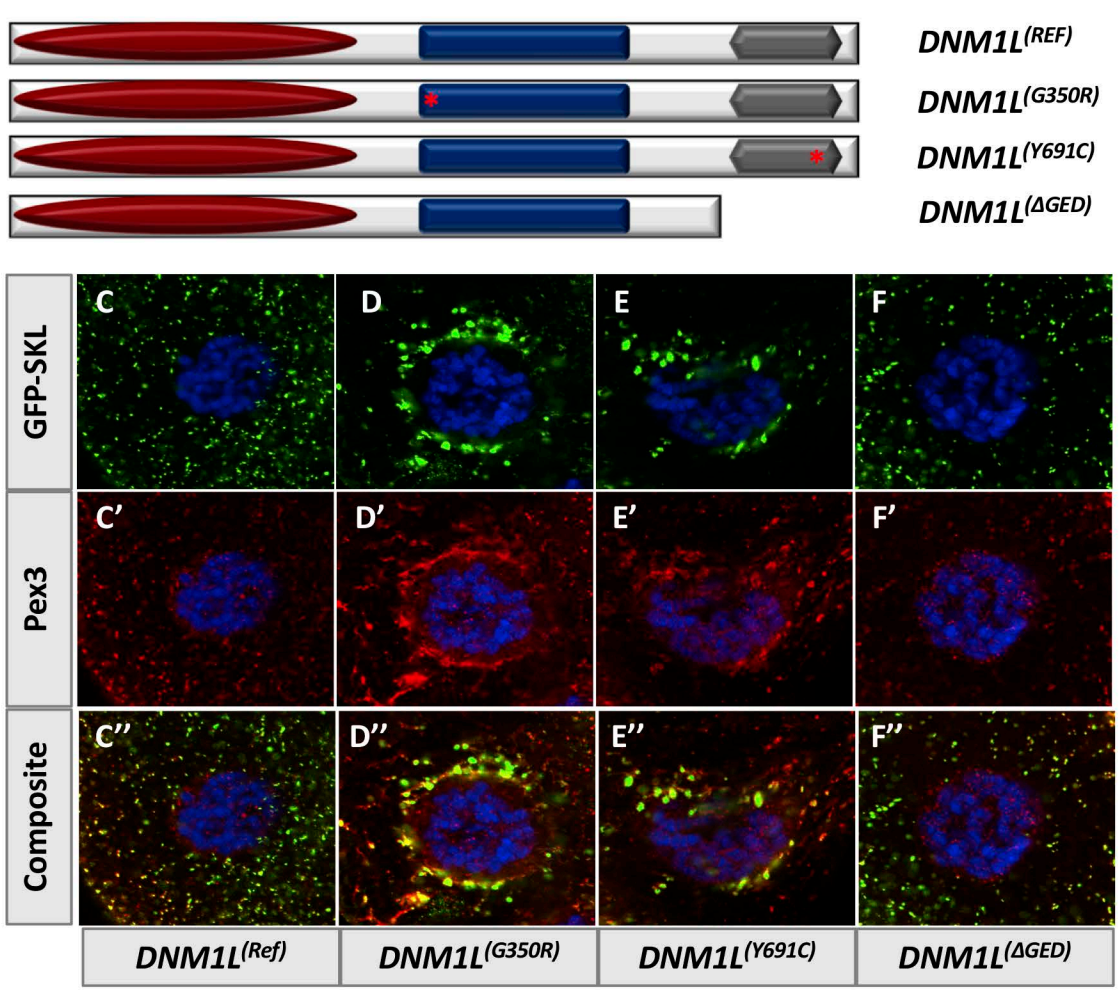

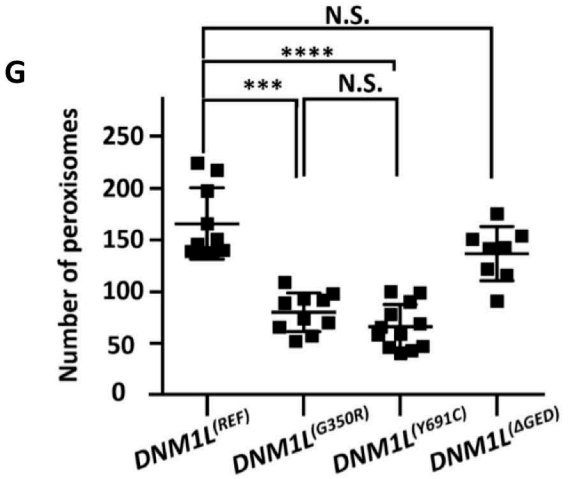

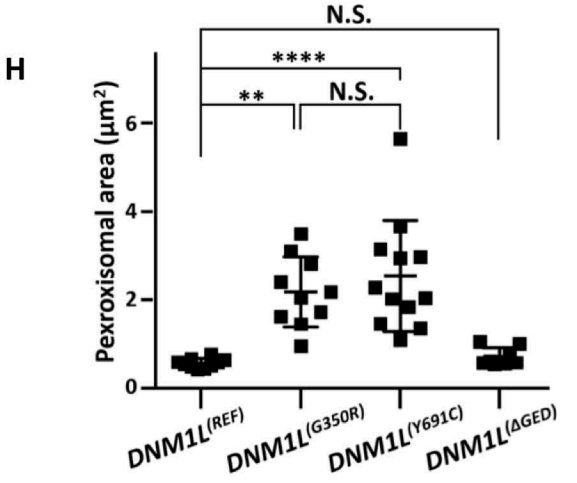

FIGURE 3

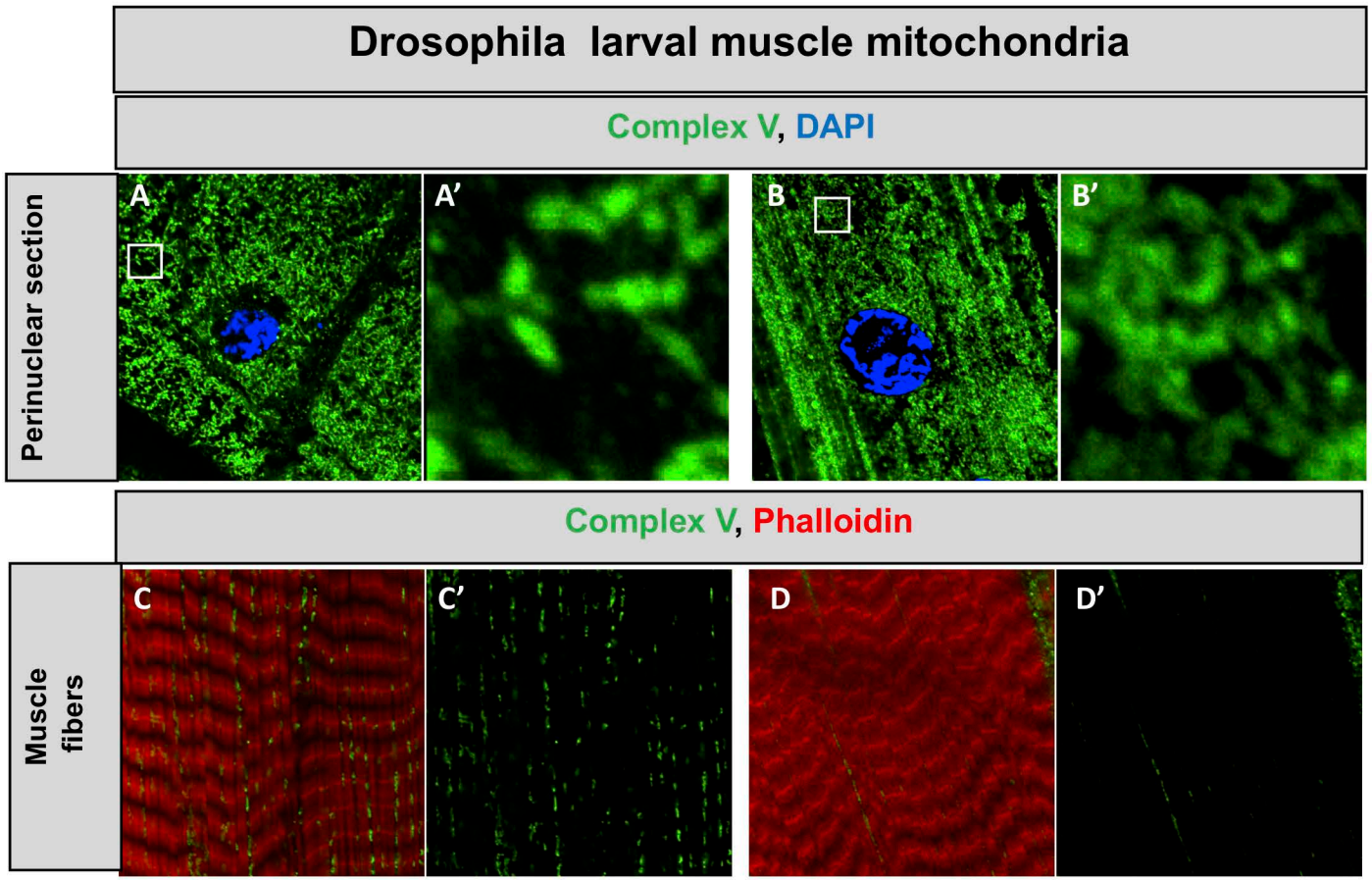
Drosophila larval muscle mitochondria
Complex V, DAPI
Perinuclear section
A
A'
B
B'
Complex V, Phalloidin
Muscle fibers
C
C'
D
D'

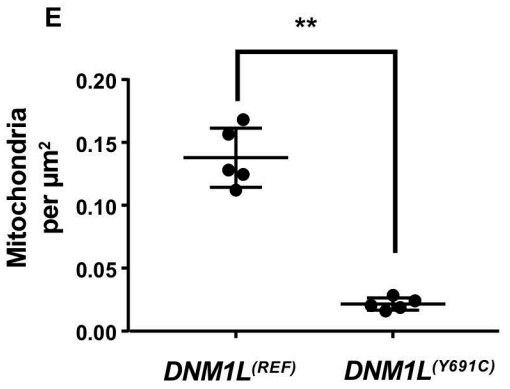
E
**
Mitochondria per µm²
0.20
0.15
0.10
0.05
0.00
DNM1L(REF)
DNM1L(Y691C)

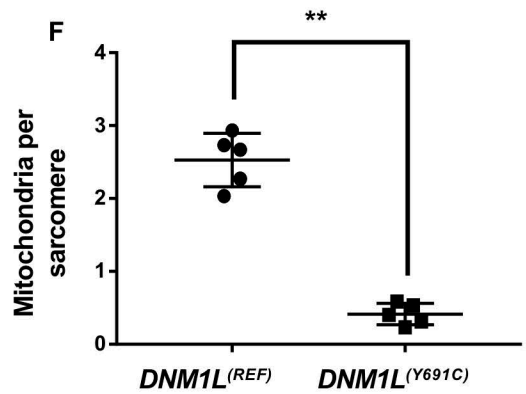
F
**
Mitochondria per sarcomere
4
3
2
1
0
DNM1L(REF)
DNM1L(Y691C)

FIGURE 4

De novo missense variant in the GTPase effector domain (GED) of DNM1L leads to static encephalopathy and seizures

Nurit Assia Batzir, Pranjali Bhagwat, Tanya Eble, et al.

Cold Spring Harb Mol Case Stud published online March 8, 2019
Access the most recent version at doi:10.1101/mcs.a003673